PHYSICAL REVIEW C **92**, 024319 (2015)

# Analogous intruder behavior near Ni, Sn, and Pb isotopes

S. N. Liddick,[1,2] W. B. Walters,[3] C. J. Chiara,[3,4,*] R. V. F. Janssens,[4] B. Abromeit,[1] A. Ayres,[5] A. Bey,[5] C. R. Bingham,[5] M. P. Carpenter,[4] L. Cartegni,[5] J. Chen,[6] H. L. Crawford,[7] I. G. Darby,[8] R. Grzywacz,[5] J. Harker,[3] C. R. Hoffman,[4] S. Ilyushkin,[9] F. G. Kondev,[6] N. Larson,[1,2] M. Madurga,[5] D. Miller,[5] S. Padgett,[5] S. V. Paulauskas,[5] M. M. Rajabali,[8] K. Rykaczewski,[10] D. Seweryniak,[4] S. Suchyta,[1,2,†] and S. Zhu[4]

[1]*National Superconducting Cyclotron Laboratory (NSCL), Michigan State University, East Lansing, Michigan 48824, USA*
[2]*Department of Chemistry, Michigan State University, East Lansing, Michigan 48824, USA*
[3]*Department of Chemistry and Biochemistry, University of Maryland, College Park, Maryland 20742, USA*
[4]*Physics Division, Argonne National Laboratory, Argonne, Illinois 60439, USA*
[5]*Department of Physics and Astronomy, University of Tennessee, Knoxville, Tennessee 37996, USA*
[6]*Nuclear Engineering Division, Argonne National Laboratory, Argonne, Illinois 60439, USA*
[7]*Nuclear Science Division, Lawrence Berkeley National Laboratory, Berkeley, California 94720, USA*
[8]*Instituut voor Kern- en Stralingsfysica, Katholieke Universiteit Leuven, B-3001 Leuven, Belgium*
[9]*Department of Physics and Astronomy, Mississippi State University, Mississippi State, Mississippi 39762, USA*
[10]*Physics Division, Oak Ridge National Laboratory, Oak Ridge, Tennessee 37831, USA*

(Received 23 October 2014; revised manuscript received 19 June 2015; published 25 August 2015)

Near shell closures, the presence of unexpected states at low energies provides a critical test of our understanding of the atomic nucleus. New measurements for the $N = 42$ isotones ${}^{69}_{27}$Co and ${}^{71}_{29}$Cu, along with recent data and calculations in the Ni isotopes, establish a full set of complementary, deformed, intruder states astride the closed-shell ${}_{28}$Ni isotopes. Nuclei with a one-proton hole or one-proton particle adjacent to $Z = 28$ were populated in $\beta$-decay experiments and in multinucleon transfer reactions. A $\beta$-decaying isomer, with a 750(250)-ms half-life, has been identified in ${}^{69}_{27}$Co$_{42}$. It likely has low spin and accompanies the previously established $7/2^-$ state. Complementary data for the levels of isotonic ${}^{71}_{29}$Cu$_{42}$ support the presence of a deformed, $\Delta J = 1$ band built on the proton intruder $7/2^-$ level at 981 keV. These data, together with recent studies of lower-mass Co and Cu isotopes and extensive work near ${}^{68}$Ni, support the view that intruder states based on particle-hole excitations accompany *all* closed proton shells with $Z \geqslant 28$.

DOI: 10.1103/PhysRevC.92.024319 PACS number(s): 21.10.−k, 23.40.−s, 23.20.Lv, 27.50.+e

The properties of the atomic nucleus are strongly influenced by the nature of individual quantum states available to its constituent protons and neutrons. The presence of periodic, large energy gaps between adjacent single-particle states leads to an inherent stability at characteristic nucleon numbers of 2, 8, 20, 28, 50, 82, and, for neutrons, 126. The fact that the element ${}_{50}$Sn has the largest number of stable isotopes (ten in all) can be attributed to the large energy gap between the $g_{9/2}$ and $g_{7/2}$ single-particle states at $Z = 50$. The enhanced stability of the so-called doubly-magic nuclei is akin to the chemical inertness of noble gases due to the complete filling of an atomic electron shell. The presence of large energy gaps forms the basis for the nuclear shell model [1,2] which has been successful in predicting a wide variety of nuclear properties by reducing the complexity of the description of a large quantum many-body system to that of an inert core of nucleons with a reduced valence space of protons and neutrons. The experimental study of nuclei adjacent to shell closures, in particular those only one nucleon away from a closure, is critical to our understanding of exotic nuclear systems [3–6]. Using the energies, spins, parities, and spectroscopic factors, it is possible to identify the single-particle states that are important for the description of a nuclear system as well as to establish their relative ordering.

The ${}_{49}$In and ${}_{51}$Sb isotopes provide an illustrative example. Naively, the level structures of odd-$A$ In (Sb) isotopes consist of a single-proton hole (particle) in the $pf$ and $g_{9/2}$ ($g_{7/2}$ and $d_{5/2}$) single-particle states. The discovery of low-energy $3/2^+$ and $1/2^+$ levels in the one-proton hole nuclei ${}^{115,117}_{49}$In$_{66,68}$ [7] associated with particle-hole excitations across the $Z = 50$ gap set off a flurry of investigations in the adjacent ${}_{49}$In, ${}_{50}$Sn, and ${}_{51}$Sb nuclei [8,9] as well as in ${}_{81}$Tl, ${}_{82}$Pb, and ${}_{83}$Bi nuclei. Such studies eventually led to the establishment of full sets of complementary, intruder states based on particle-hole excitations in both regions of $Z$ (50 and 82). These intruder states were shown to be associated with deformation, and triple-shape coexistence was reported in ${}^{186}$Pb$_{104}$ [10]. The parallel movement of the $1/2^+$ and $9/2^+$ levels of odd-$A$ ${}_{49}$In and ${}_{51}$Sb isotopes is illustrated in Fig. 1. The large degrees of deformation inferred for the intruder states in the In isotopes lend themselves to an interpretation within the Nilsson model with the low-energy levels described by an admixture of numerous spherical shell-model single-particle states. This comes with a concomitant change in the occupancies of the spherical shell-model neutron states, that is implicitly assumed when describing these intruders solely by their dominant proton character as excitations across the major shell, as is done in Fig. 1. The full scope of the experimental observables has been carefully organized in three review articles [11–13]

---

[*] Present address: Army Research Laboratory, Adelphi, MD 20783.

[†] Present address: Department of Nuclear Engineering, University of California–Berkeley, Berkeley, CA 94720.

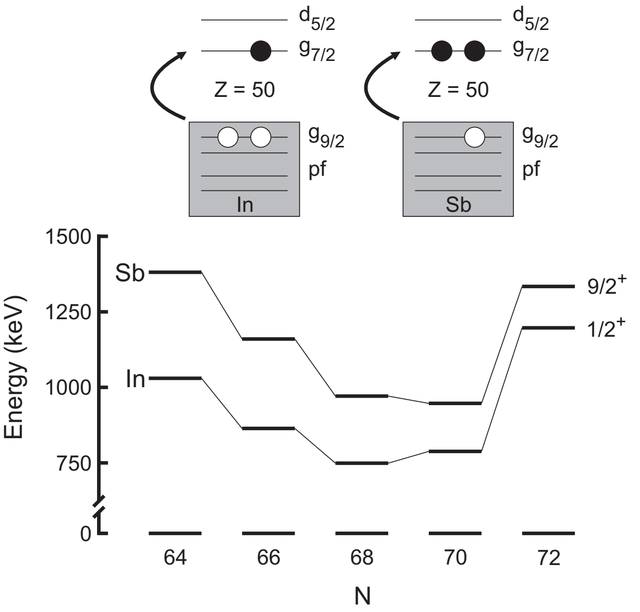

FIG. 1. Top: Single-particle level ordering for the In and Sb isotopes. Normal proton configurations in In (Sb) consist of a proton hole (particle) below (above) $Z = 50$. Schematic particle-hole excitations in the In and Sb isotopes are also shown; see text for details. Bottom: The energies of the Sb $9/2^+$ and In $1/2^+$ intruder levels plotted with respect to their respective ground states. The experimentally observed spins and parities of the intruder states are obtained from the projection of the angular momentum on the symmetry axis.

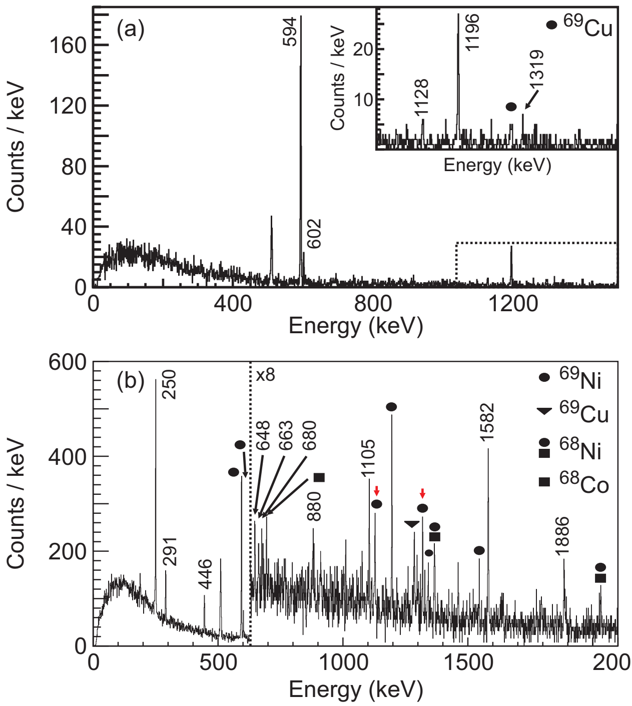

FIG. 2. (Color online) (a) $\beta$-delayed $\gamma$ rays detected within one second of the arrival of a $^{69}$Co ion at the experimental station. The transitions in $^{69}$Ni are marked by their respective energies. Inset: $\gamma$-ray energy spectrum between 1040 and 1500 keV. The circle indicates a transition assigned in $^{69}$Cu following the decay of $^{69}$Ni [24]. (b) $\beta$-delayed $\gamma$-ray transitions identified within one second of the arrival of a $^{69}$Fe ion. Transitions attributed to the decay of $^{69}$Fe are marked by their respective energies. Arrows mark the locations of the $^{69}$Co $\beta$-delayed $\gamma$ rays at 1128 and 1319 keV.

focusing heavily on intruder states associated with the Pb and Sn closed shells.

Noticeably absent in the recent review of Ref. [11] is a discussion of proton intruder states in $_{27}$Co and $_{29}$Cu nuclei. The possibility of an intruder structure in $^{69}$Cu$_{40}$ analogous to the above cases had been suggested [14,15], but data demonstrating a full sequence of proton intruder levels was not available. Herein, new data are presented for the $N = 42$ isotones $^{69}$Co and $^{71}$Cu. They establish a sequence of complementary intruder structures for odd-$Z$ $_{27}$Co and $_{29}$Cu nuclei, with a single hole and single particle, respectively, adjacent to the $Z = 28$ closed proton shell. The present results can be combined with the recent interpretation of the structure of the 1868-keV, $2_2^+$ level in $^{70}$Ni$_{42}$, that sits between $^{69}$Co$_{42}$ and $^{71}$Cu$_{42}$, as a member of a deformed intruder band [16]. This has also recently been suggested by theory [17]. As such, these are the first new complementary proton particle-hole excitation sequences established in the past 30 years. The data support the view that deformed intruder configurations based on particle-hole excitations are a general feature characterizing structure near all proton closed shells with $Z \geqslant 28$.

The details of the experimental system have been published previously [18–20], and only the salient features are reproduced here. Ions of $^{69}$Fe and $^{69}$Co were produced by impinging a 140-MeV/$A$ $^{86}$Kr primary beam on a $^9$Be target. The fragmentation products were separated, identified, and delivered to the Beta Counting System (BCS) [21] surrounded by the Segmented Germanium Array (SeGA) [22] and read out using the NSCL Digital Data Acquisition System (DDAS) [23].

The $\beta$ decay of $^{69}$Co to $^{69}$Ni, studied previously [6], was monitored in the present experiment. This decay leads to three strong $\gamma$ rays at 1196, 602, and 594 keV which can be observed in Fig. 2(a). All three transitions lead to the $1/2^-$ isomeric state at 321 keV in $^{69}$Ni which, subsequently, decays to $^{69}$Cu ($t_{1/2} = 3500$ ms [24]). The $^{69}$Co decay curve measured in coincidence with the 594-keV transition was fit with contributions from the decay of $^{69}$Co and a constant background to yield a half-life of 180(20) ms; see Fig. 3(a). Without the $\gamma$-ray coincidence requirement, the $^{69}$Co decay curve yields a half-life of 206(20) ms. Previously reported $^{69}$Co half-life values without the $\gamma$-ray coincidence include 229(24) [25], 220(20) [6], 170(30) [26], and 270(50) ms [27].

The decay of $^{69}$Co was also studied as the daughter product of independently produced $^{69}$Fe through the $^{69}\text{Fe} \rightarrow {}^{69}\text{Co} \rightarrow {}^{69}\text{Ni}$ chain. A total of ten $\gamma$ rays are assigned to the $\beta$ decay of $^{69}$Fe observed in Fig. 2(b).

For the three most intense low-energy transitions, 250, 291, and 446 keV, $\gamma$-gated decay curves were extracted and fit with a single exponential and a constant background. The half-lives are consistent with each other within error and a half-life of 162(7) ms is adopted for the $\beta$ decay of $^{69}$Fe [see

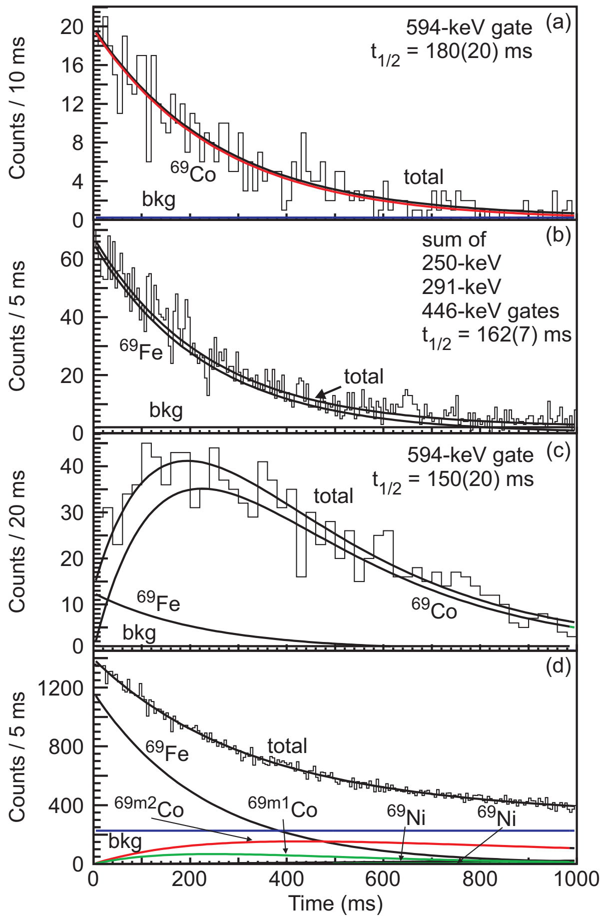

FIG. 3. (Color online) (a) Decay curve in coincidence with the 594-keV transition following the decay of directly produced $^{69}$Co, fit with an exponential decay and a constant background. (b) Sum of the $^{69}$Fe decay curves generated from gates placed on the 250-, 291-, and 446-keV transitions fit with an exponential decay and constant background. (c) Decay curve in coincidence with the 594-keV transition following the decay of $^{69}$Co produced from $^{69}$Fe. The curve is fit with the growth and decay of $^{69}$Co and two background components. (d) The total decay curve for $^{69}$Fe with components attributed to the decay of $^{69}$Fe, two states in $^{69}$Co, $^{69}$Ni, and a constant background. The grow-in and decay curve for $^{69}$Ni is explicitly separated into two components corresponding to the two $^{69}$Co $\beta$-decaying states.

Fig. 3(b)], which is longer than previously reported [25,28]. If the $\gamma$-ray coincidence requirement is removed and the half-life refit using the assumptions of Ref. [28], the resulting half-life is consistent with that reported in Refs. [25,28].

The 594-keV $\gamma$ ray was observed following the decay of $^{69}$Co populated through $^{69}$Fe decay. The 594-keV coincident decay curve displayed the characteristic growth and decay of a daughter activity [see Fig. 3(c)]. Fitting this curve with the Bateman equations for growth and decay and two background components (one for Compton-scattered $^{69}$Fe $\gamma$ rays and the other constant) resulted in a $^{69}$Co half-life of 150(20) ms, lower still than the half-life determined above from the decay of independently produced $^{69}$Co.

TABLE I. $\gamma$-ray energies and absolute intensities following the decay of $^{69}$Co from the present work compared to previous literature values.

| $E$ (keV) | Intensity (%) | | |
|---|---|---|---|
| | Present work fragmentation | Present work $\beta$ decay | Ref. [6] |
| 594.2 (4) | 42(4) | 16(2) | 56.7(47) |
| 602.4 (4) | 4.4 (12) | 1.7(5) | 8.9(12) |
| 1128.5 (5) | 2.6 (11) | 1.0(5) | 8.3(13) |
| 1196.3 (4) | 9.0 (20) | 3.5(8) | 11.2(16) |
| 1319 (1) | 0.6 (3) | 2.7 (7) | 9.2(14) |

The total decay curve for $^{69}$Fe is shown in Fig. 3(d). It was not possible to fit this curve solely with contributions from $^{69}$Fe (162 ms), $^{69}$Co (180 ms), and a constant background. If the half-life of $^{69}$Fe is fixed to 162 ms, the $^{69}$Co half-life required for an acceptable fit is greater than 500 ms, more than a factor of 2 larger than measured in the decay of $^{69}$Co produced in fragmentation. The inconsistencies in the $^{69}$Co $\beta$-decay half-lives require the presence of an additional $\beta$-decaying state along the $^{69}$Fe $\rightarrow$ $^{69}$Co $\rightarrow$ $^{69}$Ni chain. In principle, this longer-lived state can be placed in either $^{69}$Fe or $^{69}$Co. However, if it is assumed to be in $^{69}$Fe, with a single $\beta$-decaying state in $^{69}$Co, the absolute intensities of the $^{69}$Co $\beta$-delayed transitions should be identical between the data presented above and previous studies [6]. Table I presents absolute intensities extracted based on the observed $\gamma$-ray intensities, the absolute efficiency of SeGA, the number of $\beta$-decay electrons attributed to $^{69}$Co, and the total number of ions produced.

Inspection of Table I reveals inconsistent values for the absolute intensity of the $\beta$-delayed transitions from $^{69}$Co across the three studies. The $\gamma$ rays reported by Mueller *et al.* [6], at 1128, 1319, 1343, 1545, and 1642 keV, but not placed in their $^{69}$Ni level scheme, are observed in Fig. 2(b) but barely, if at all, in the decay spectrum of directly produced $^{69}$Co. As a result, the presence of multiple $\beta$-decaying states in $^{69}$Co is proposed. It is suggested that the study of Ref. [6] observed the production and decay of *both* isomers. The half-life of 180(20) ms is adopted for one of the $\beta$-decaying states in $^{69}$Co, based on the similarity of the half-lives extracted from the directly produced $^{69}$Co decay curves with and without a 594-keV $\gamma$-ray coincidence requirement. Any contamination from the longer-lived activity in the directly produced $^{69}$Co would lower the adopted half-life value for the short-lived state. Using both the $^{69}$Fe and $^{69}$Co half-lives results in the requirement for a longer-lived, 750(250)-ms, $^{69}$Co state.

The level structure of $^{69}$Ni was established by both the $\beta$ decay of $^{69}$Co [6] and the isomeric decay of the $17/2^-$ state [29]. The salient features include a ground state associated with a $\nu g_{9/2}$ configuration, an isomeric level at 321 keV of $\nu p_{1/2}^{-1}$ character, and a $\nu f_{5/2}^{-1}$ state at 915 keV that decays to the $1/2^-$ isomeric state via the 594-keV transition. The short-lived $^{69}$Co level has been assigned a $7/2^-$ spin and parity, based on the

$\pi f_{7/2}^{-1}$ configuration observed in all other odd-$A$ Co isotopes, a log $ft$ value to the $5/2^-$ state in $^{69}$Ni consistent with an allowed decay, and the lack of an observed $\beta$-decay branch to the $1/2^-$ isomeric state at 321 keV. A second $\beta$-decaying state in $^{69}$Co must have $\Delta J \geqslant 3$ to account for the observed isomerism. The much larger relative intensities of the $\gamma$ rays at 1128 and 1319 keV in the $^{69}\text{Fe} \rightarrow ^{69}\text{Co} \rightarrow ^{69}\text{Ni}$ chain compared to the decay of directly produced $^{69}$Co suggest a low spin for the levels depopulated by these two $\gamma$ rays. The fact that these two transitions are not observed in the decay sequence of the $17/2^-$ isomer supports this conclusion. Hence, a low spin is assigned for the proposed 750-ms isomer. A tentative $1/2^-$ level is known in both $^{65}$Co [30] and $^{67}$Co [31] at 1095 and 492 keV, respectively, which is attributed to proton excitations across the $Z = 28$ shell. Thus, the longer-lived $\beta$-decaying isomer in $^{69}$Co is, tentatively, proposed to correspond to a low-energy $(1/2^-)$ state similar to $^{65,67}$Co.

Limits can be placed on the energy of this supposed $1/2^-$ state relative to the $7/2^-$ level, based on the $M3$, $1/2^- \rightarrow 7/2^-$ transition in neighboring $^{67}$Co [31]. Assuming that the $M3$ strength for the $1/2^- \rightarrow 7/2^-$ transition is the same in $^{67}$Co and $^{69}$Co, the energy difference above which the state would decay strictly through $\gamma$-ray emission can be determined. The $\gamma$-ray branch in $^{67}$Co is taken as 80% [31]. Solely for the purpose of establishing this limit, using a $\gamma$-ray branch in $^{69}$Co of 100% for the $1/2^- \rightarrow 7/2^-$ transition implies an energy separation of 467 keV. If the energy separation is greater than this value, the decay of the state should proceed through $\gamma$-ray emission. Since only the $\beta$-decay emission has been observed, either the energy separation is lower than this value or the strength of this transition in $^{69}$Co is not the same as in $^{67}$Co. To provide another point of reference, if the transition strength is lowered by an order magnitude corresponding with some of the weakest known $M3$ transitions in this region [32], then the energy difference is 661 keV. Unfortunately, it is not possible to determine the relative order of the two $\beta$-decaying states, based on the current data.

In previous studies of excitations in $^{71}\text{Cu}_{42}$ populated by $\beta$ decay [33], fragmentation [29], and multi-nucleon transfer [34], $11/2^-$ and $9/2^-$ levels were identified on top of a $7/2^-$ state at 981 keV that could be interpreted as the head of an intruder band [15], in analogy with the sequences reported in $^{67}$Cu [35]. Identification as a possible intruder band head was strengthened somewhat when another low-energy $7/2^-$ level at 1189 keV was populated in Coulomb excitation [36]. Recently, the lifetimes of both these $7/2^-$ states were determined [37] and a rather large $B(E2)$ value [44(2) $e^2\text{fm}^4$] was found for the 981-keV line, even though it is roughly one fourth that of the 1189-keV transition. This rather large $B(E2)$ value for the 981-keV transition seems to argue against a single-hole character for this $7/2^-$ state, with its hindrance with respect to the 1189-keV transition possibly due to the nature of the $^{71}$Cu ground state [38]. New levels associated with the band starting at 981 keV have now been identified in a multinucleon transfer reaction between $^{70}$Zn and $^{208}$Pb presented herein. The details of the experiment have been reported in previous work—in particular, that reporting a study of $^{68}$Ni levels [39]—and are only briefly summarized here. Excited states in odd-$A$ Cu isotopes were populated using reactions of a 440-MeV $^{70}$Zn beam on a 50 mg/cm$^2$ $^{208}$Pb target located at the center of the Gammasphere array [40]. Beam pulses were separated by 412 ns and were approximately 0.3 ns wide. The data were accumulated using a minimum $\gamma$-ray coincidence requirement of 2 or 3; see Ref. [39] for additional details. Four new transitions were identified and organized as given in Fig. 4, extending the sequence on top of the $7/2^-$ level from $11/2^-$ to $(17/2^-)$. Thus, this observation confirms the presence of an intruder band of sizable deformation, built on a $7/2^-$ level that can be associated with a $7/2^-[303]$ Nilsson state.

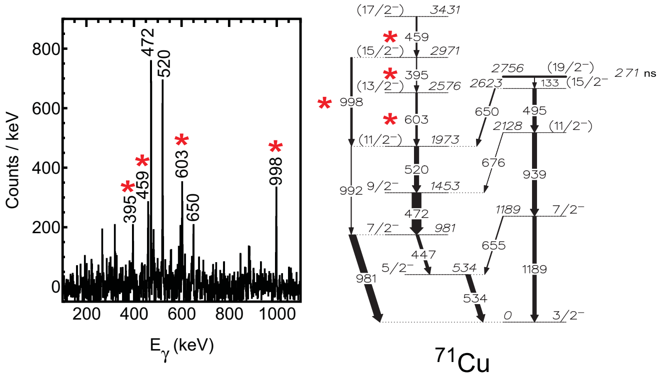

FIG. 4. (Color online) Location of the $\gamma$ rays identified in the present work in the level scheme of $^{71}$Cu, establishing the band to a spin of $(17/2^-)$. The lifetime of the 2756-keV $19/2^-$ state was taken from [29].

It is now possible to interpret these data as key to establishing a fully complementary set of proton intruder levels near $_{28}$Ni, when combined with recent experimental studies of both $^{65,67}\text{Co}_{38,40}$, where tentative low-energy $1/2^-$ levels had already been identified [30,31], and $^{67,69}\text{Cu}_{38,40}$, where $\Delta J = 1$ sequences had been reported [14,35,41,42]. The systematics of the proton intruder levels in this region can be found in Fig. 5. Again, analogous to Fig. 1, the schematic proton excitations across the $Z = 28$ shell presented in Fig. 5 provide the expected, dominant proton configurations of the intruder states with the qualification that the neutron occupancies are altered from their simple, spherical shell-model occupancies. A dramatic drop in the excitation energy of the intruding $7/2^-$ level by roughly 1.4 MeV is observed between $^{67}\text{Cu}_{38}$ and $^{71}\text{Cu}_{42}$. A parallel decrease is seen for the $(1/2^-)$ level in the Co isotopes between $N = 38$ and $N = 40$. If the energy reduction follows the same trend as that found in the Cu isotopes, it could lead to an inversion in the order of the $7/2^-$ and $1/2^-$ states in $^{69}$Co. Sieja and Nowacki suggested [43] that while the simple two-particle one-hole proton excitations shown at the top of Fig. 5 are a reasonable description for $^{67,69}\text{Cu}_{38,40}$, they cannot account for the significantly lowered position of the 981-keV $7/2^-$ level in $^{71}\text{Cu}_{42}$. Instead, they indicate a more deformed structure, such as a Nilsson framework, provides a better description which is also consistent with the lower position of the prolate $0_2^+$ level in isotonic $^{70}\text{Ni}_{42}$. The Nilsson $K = 1/2^-$ [321] configuration previously assigned to the $1/2^-$ isomer

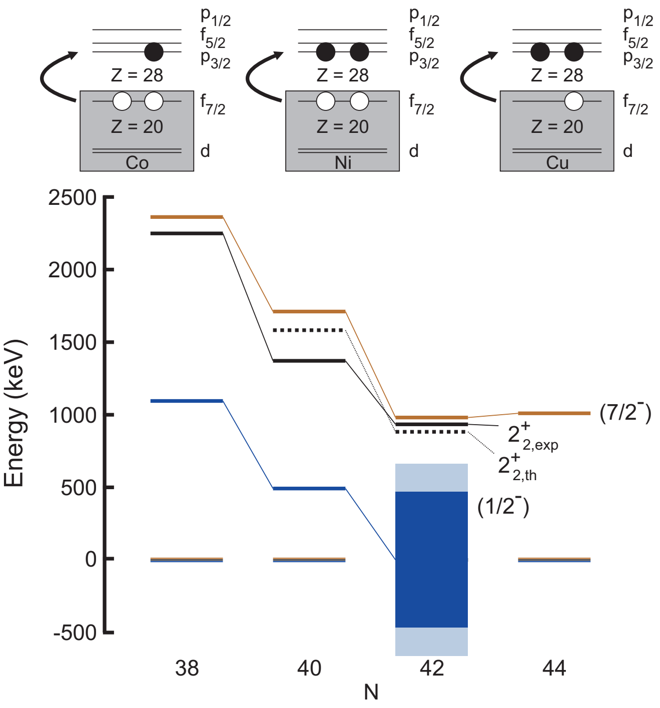

FIG. 5. (Color online) (top) Single-particle level ordering for the Co and Cu isotopes. "Normal" proton configurations in Co (Cu) consist of a proton hole (particle) below (above) $Z = 28$. Schematic particle-hole excitations in the Co, Ni, and Cu isotopes are also shown; see text for details. The experimentally observed spins and parities of the deformed intruder states are obtained from the projection of the angular momentum on the symmetry axis. (bottom) The energies of the Cu $(7/2^-)$ (copper-colored) and Co $(1/2^-)$ (blue) intruder levels with respect to their ground states. The energy of the Co intruder states were taken from Refs. [30,31]. The range of values for the energy difference between the two states in $^{69}$Co were determined from two different assumptions for the strength of the unobserved $M3$ $\gamma$-ray transition; see text for details. The energies of the experimentally observed intruding $2^+$ levels in the even-even Ni isotopes are shown divided by two (black solid line) along with theoretical calculations (black dashed line) [17,47].

in $^{67}$Co$_{40}$ is seemingly also appropriate for the $\beta$-decaying low-spin isomer in $^{69}$Co$_{42}$.

The major experimental and theoretical strides made recently in the study of the even $^{66,68,70}$Ni$_{38,40,42}$ nuclei are of equal importance. Detailed data for $^{68}$Ni have been reported [39,44–46] and are complemented by new Monte Carlo shell model (MCSM) calculations [47,48] with the A3DA effective interaction [47], which explicitly allows for proton excitations across the $Z = 28$ shell. Proton intruder configurations manifesting as low-energy excited $0^+$ states have been observed or suggested in all three $^{66,68,70}$Ni isotopes [16,46,49]. Deformed bands built on top of these $0^+$ intruder states have been proposed and the associated $2^+$ band members are compared, in Fig. 5, to the tentative $1/2^-$ and $7/2^-$ levels in Co and Cu, respectively, after dividing the $2^+$ energies by a factor of 2 to roughly accommodate the difference between the two-particle–two-hole excitation in Ni and the particle-hole one in either Cu or Co. The MCSM calculations are able to reproduce the drop in the energy of the proton intruder $2^+$ states in $^{68,70}$Ni. Inspection of the $2^+$ state wave functions reveals that these states are members of strongly prolate-deformed rotational bands [17] in both nuclei. It should also be noted that shape coexistence was identified in both $^{66,68}$Ni in global calculations [32] which did not, however, identify $^{70}$Ni as possessing a strong prolate-deformed minimum.

The systematics of the proton intruder levels near $Z = 28$ of Fig. 5 compare favorably with the behavior seen in both the $Z \sim 50$ In, Sn, and Sb isotopes (Fig. 1) and the $Z \sim 82$, Tl, Pb, and Bi region. In all three areas of the nuclear chart, a parabolic decrease of the intruder state excitation energy is observed and a minimum is reached midway slightly above the midpoint between the neutron closed shells at $N = 42$ for the Co, Ni, and Cu region. The MCSM calculations predict triple shape coexistence in $^{68}$Ni involving spherical, prolate, and oblate configurations. The situation parallels the development of triple shape coexistence in $^{186}$Pb [10]. Thus, the proton intruder states identified in the Co, Ni, and Cu region appear to be linked to the presence of shape coexistence. Furthermore, the present results are in line with other studies presenting evidence for shape coexistence in this region, based on high-spin levels in Cr and Fe isotopes [50], and additional investigations pointing to a systematic maximum in collectivity along $N = 42$ isotones below Ni [51], though measurements are still needed in the $N = 44$ isotones of Cr, Fe, Co, and Cu.

In summary, proton particle-hole intruder states originating from excitations across $Z = 28$ were identified in the $N = 42$ isotones $^{69}$Co and $^{71}$Cu. These new data along with the MCSM calculations provide the key pieces of information to reinterpret the region around the Ni isotopes in terms of spherical-deformed shape coexistence originating from particle-hole excitations. The Ni region now exhibits similar patterns to those observed in heavier Sn and Pb isotopes herewith suggesting the ubiquitous nature of these types of excitations for closed proton shells with $Z \geqslant 28$. The implications are that structures similar to those observed near $^{116}$Sn$_{66}$, $^{186}$Pb$_{104}$, and now $^{68}$Ni$_{40}$, can also be expected [17] at midshell for heavier Sn and Pb nuclei near $N = 104$ and $N = 154$, respectively.

## ACKNOWLEDGMENTS

This material is based upon work supported by the National Science Foundation under Contract No. NSF-06067007 (NSCL), the US Department of Energy, National Nuclear Security Administration under Grant No. DE-FC03-03NA00143, and Award No. DE-NA0000979, the U.S. Department of Energy, Office of Science, Office of Nuclear Physics, under Grants No. DE-FG02-94ER40834 (Maryland), No. DE-FG02-96ER40983 (UT), No. DE-AC05-060R23100 (ORAU), and under Contracts No. DE-AC02-06CH11357 (ANL) and No. DE-AC05-00OR22725 (ORNL). This research used resources of ANL's ATLAS facility, which is a DOE Office of Science User Facility.

[1] M. G. Mayer, Phys. Rev. **75**, 1969 (1949).

[2] O. Haxel, J. H. D. Jensen, and H. E. Suess, Phys. Rev. **75**, 1766 (1949).

[3] J. M. Allmond, A. E. Stuchbery, J. R. Beene, A. Galindo-Uribarri, J. F. Liang, E. Padilla-Rodal, D. C. Radford, R. L. Varner, A. Ayres, J. C. Batchelder, A. Bey, C. R. Bingham, M. E. Howard, K. L. Jones, B. Manning, P. E. Mueller, C. D. Nesaraja, S. D. Pain, W. A. Peters, A. Ratkiewicz, K. T. Schmitt, D. Shapira, M. S. Smith, N. J. Stone, D. W. Stracener, and C.-H. Yu, Phys. Rev. Lett. **112**, 172701 (2014).

[4] K. L. Jones, A. S. Adekola, D. Bardayan, J. Blackmon, K. Chae, K. A. Chipps, J. Cizewski, L. Erikson, C. Harlin, R. Hatarik, R. Kapler, R. Kozub, J. Liang, Z. M. R. Livesay, B. Moazen, C. Nesaraja, F. Nunes, S. Pain, N. Patterson, D. Shapira, J. Shriner, M. Smith, T. Swan, and J. Thomas, Nature (London) **465**, 454 (2010).

[5] K. T. Flanagan, P. Vingerhoets, M. Avgoulea, J. Billowes, M. L. Bissell, K. Blaum, B. Cheal, M. De Rydt, V. N. Fedosseev, D. H. Forest, C. Geppert, U. Köster, M. Kowalska, J. Krämer, K. L. Kratz, A. Krieger, E. Mané, B. A. Marsh, T. Materna, L. Mathieu, P. L. Molkanov, R. Neugart, G. Neyens, W. Nörtershäuser, M. D. Seliverstov, O. Serot, M. Schug, M. A. Sjoedin, J. R. Stone, N. J. Stone, H. H. Stroke, G. Tungate, D. T. Yordanov, and Y. M. Volkov, Phys. Rev. Lett. **103**, 142501 (2009).

[6] W. F. Mueller, B. Bruyneel, S. Franchoo, H. Grawe, M. Huyse, U. Köster, K.-L. Kratz, K. Kruglov, Y. Kudryavtsev, B. Pfeiffer, R. Raabe, I. Reusen, P. Thirolf, P. Van Duppen, J. Van Roosbroeck, L. Vermeeren, W. B. Walters, and L. Weissman, Phys. Rev. Lett. **83**, 3613 (1999).

[7] A. Bácklin, B. Fogelberg, and S. Malmskog, Nucl. Phys. A **96**, 539 (1967).

[8] W. Dietrich, A. Bäcklin, C. Lannergård, and I. Ragnarsson, Nucl. Phys. A **253**, 429 (1975).

[9] R. L. Auble, J. B. Ball, and C. B. Fulmer, Phys. Rev. **169**, 955 (1968).

[10] A. N. Andreyev, M. Huyse, P. Van Duppen, L. Weissman, D. Ackermann, J. Gerl, F. P. Hessberger, S. Hofmann, A. Kleinbohl, G. Munzenberg, S. Reshitko, C. Schlegel, H. Schaffner, P. Cagarda, M. Matos, S. Saro, A. Keenan, C. Moore, C. D. O'Leary, R. D. Page, M. Taylor, H. Kettunen, M. Leino, A. Lavrentiev, R. Wyss, and K. Heyde, Nature (London) **405**, 430 (2000).

[11] K. Heyde and J. L. Wood, Rev. Mod. Phys. **83**, 1467 (2011).

[12] J. L. Wood, K. Heyde, W. Nazarewicz, M. Huyse, and P. van Duppen, Phys. Rep. **215**, 101 (1992).

[13] K. Heyde, P. V. Isacker, M. Waroquier, J. Wood, and R. Meyer, Phys. Rep. **102**, 291 (1983).

[14] T. Ishii, M. Asai, A. Makishima, I. Hossain, M. Ogawa, J. Hasegawa, M. Matsuda, and S. Ichikawa, Phys. Rev. Lett. **84**, 39 (2000).

[15] A. Oros-Peusquens and P. Mantica, Nucl. Phys. A **669**, 81 (2000).

[16] C. J. Chiara, D. Weisshaar, R. V. F. Janssens, Y. Tsunoda, T. Otsuka, J. L. Harker, W. B. Walters, F. Recchia, M. Albers, M. Alcorta, V. M. Bader, T. Baugher, D. Bazin, J. S. Berryman, P. F. Bertone, C. M. Campbell, M. P. Carpenter, J. Chen, H. L. Crawford, H. M. David, D. T. Doherty, A. Gade, C. R. Hoffman, M. Honma, F. G. Kondev, A. Korichi, C. Langer, N. Larson, T. Lauritsen, S. N. Liddick, E. Lunderberg, A. O. Macchiavelli, S. Noji, C. Prokop, A. M. Rogers, D. Seweryniak, N. Shimizu, S. R. Stroberg, S. Suchyta, Y. Utsuno, S. J. Williams, K. Wimmer, and S. Zhu, Phys. Rev. C **91**, 044309 (2015).

[17] Y. Tsunoda, T. Otsuka, N. Shimizu, M. Honma, and Y. Utsuno, Phys. Rev. C **89**, 031301 (2014).

[18] S. N. Liddick, B. Abromeit, A. Ayres, A. Bey, C. R. Bingham, B. A. Brown, L. Cartegni, H. L. Crawford, I. G. Darby, R. Grzywacz, S. Ilyushkin, M. Hjorth-Jensen, N. Larson, M. Madurga, D. Miller, S. Padgett, S. V. Paulauskas, M. M. Rajabali, K. Rykaczewski, and S. Suchyta, Phys. Rev. C **87**, 014325 (2013).

[19] S. N. Liddick, B. Abromeit, A. Ayres, A. Bey, C. R. Bingham, M. Bolla, L. Cartegni, H. L. Crawford, I. G. Darby, R. Grzywacz, S. Ilyushkin, N. Larson, M. Madurga, D. Miller, S. Padgett, S. Paulauskas, M. M. Rajabali, K. Rykaczewski, and S. Suchyta, Phys. Rev. C **85**, 014328 (2012).

[20] S. N. Liddick, S. Suchyta, B. Abromeit, A. Ayres, A. Bey, C. R. Bingham, M. Bolla, M. P. Carpenter, L. Cartegni, C. J. Chiara, H. L. Crawford, I. G. Darby, R. Grzywacz, G. Gürdal, S. Ilyushkin, N. Larson, M. Madurga, E. A. McCutchan, D. Miller, S. Padgett, S. V. Paulauskas, J. Pereira, M. M. Rajabali, K. Rykaczewski, S. Vinnikova, W. B. Walters, and S. Zhu, Phys. Rev. C **84**, 061305 (2011).

[21] J. I. Prisciandaro, A. C. Morton, and P. F. Mantica, Nucl. Instrum. Methods Phys. Res. Sect. A **505**, 140 (2003).

[22] W. F. Mueller, J. A. Church, T. Glasmacher, D. Gutknecht, G. Hackman, P. G. Hansen, Z. Hu, K. L. Miller, and P. Quirin, Nucl. Instrum. Methods Phys. Res. Sect. A **466**, 492 (2001).

[23] C. Prokop, S. Liddick, B. Abromeit, A. Chemey, N. Larson, S. Suchyta, and J. Tompkins, Nuc. Instrum. Methods Phys. Res. Sect. A **741**, 163 (2014).

[24] J. I. Prisciandaro, P. F. Mantica, A. M. Oros-Peusquens, D. W. Anthony, M. Huhta, P. A. Lofy, and R. M. Ronningen, Phys. Rev. C **60**, 054307 (1999).

[25] J. M. Daugas, I. Matea, J.-P. Delaroche, M. Pfutzner, M. Sawicka, F. Becker, G. Belier, C. R. Bingham, R. Borcea, E. Bouchez, A. Buta, E. Dragulescu, G. Georgiev, J. Giovinazzo, M. Girod, H. Grawe, R. Grzywacz, F. Hammache, F. Ibrahim, M. Lewitowicz, J. Libert, P. Mayet, V. Meot, F. Negoita, F. de Oliveira Santos, O. Perru, O. Roig, K. Rykaczewski, M. G. Saint-Laurent, J. E. Sauvestre, O. Sorlin, M. Stanoiu, I. Stefan, Ch. Stodel, Ch. Theisen, D. Verney, and J. Zylicz, Phys. Rev. C **83**, 054312 (2011).

[26] O. Sorlin, C. Donzaud, L. Axelsson, M. Belleguic, R. Baraud, C. Borcea, G. Canchel, E. Chabanat, J. Daugas, A. Emsallem, D. Guillemaud-Mueller, K.-L. Kratz, S. Leenhardt, M. Lewitowicz, C. Longour, M. Lopez, F. de Oliveira Santos, L. Petizon, B. Pfeiffer, F. Pougheon, M. Saint-Laurent, and J. Sauvestre, Nucl. Phys. A **660**, 3 (1999).

[27] M. Bernas, P. Armbruster, S. Czajkowski, H. Faust, J. P. Bocquet, and R. Brissot, Phys. Rev. Lett. **67**, 3661 (1991).

[28] C. Mazzocchi, R. Surman, R. Grzywacz, J. C. Batchelder, C. R. Bingham, D. Fong, J. H. Hamilton, J. K. Hwang, M. Karny, W. Królas, S. N. Liddick, P. F. Mantica, A. C. Morton, W. F. Mueller, K. P. Rykaczewski, M. Steiner, A. Stolz, J. A. Winger, and I. N. Borzov, Phys. Rev. C **88**, 064320 (2013).

[29] R. Grzywacz, R. Béraud, C. Borcea, A. Emsallem, M. Glogowski, H. Grawe, D. Guillemaud-Mueller, M. Hjorth-Jensen, M. Houry, M. Lewitowicz, A. C. Mueller, A. Nowak, A. Płochocki, M. Pfützner, K. Rykaczewski, M. G. Saint-Laurent, J. E. Sauvestre, M. Schaefer, O. Sorlin, J. Szerypo, W. Trinder, S. Viteritti, and J. Winfield, Phys. Rev. Lett. **81**, 766 (1998).

[30] D. Pauwels, O. Ivanov, N. Bree, J. Büscher, T. E. Cocolios, M. Huyse, Y. Kudryavtsev, R. Raabe, M. Sawicka, J. Van de Walle, P. Van Duppen, A. Korgul, I. Stefanescu, A. A. Hecht, N. Hoteling, A. Wöhr, W. B. Walters, R. Broda, B. Fornal, W. Krolas, T. Pawlat, J. Wrzesinski, M. P. Carpenter, R. V. F. Janssens, T. Lauritsen, D. Seweryniak, S. Zhu, J. R. Stone, and X. Wang, Phys. Rev. C **79**, 044309 (2009).

[31] D. Pauwels, O. Ivanov, N. Bree, J. Büscher, T. E. Cocolios, J. Gentens, M. Huyse, A. Korgul, Y. Kudryavtsev, R. Raabe, M. Sawicka, I. Stefanescu, J. Van de Walle, P. Van den Bergh, P. Van Duppen, and W. B. Walters, Phys. Rev. C **78**, 041307 (2008).

[32] P. Möller, A. Sierk, R. Bengtsson, H. Sagawa, and T. Ichikawa, At. Data Nucl. Data Tables **98**, 149 (2012).

[33] S. Franchoo, M. Huyse, K. Kruglov, Y. Kudryavtsev, W. F. Mueller, R. Raabe, I. Reusen, P. Van Duppen, J. Van Roosbroeck, L. Vermeeren, A. Wöhr, H. Grawe, K.-L. Kratz, B. Pfeiffer, and W. B. Walters, Phys. Rev. C **64**, 054308 (2001).

[34] T. Ishii, M. Asai, I. Hossain, P. Kleinheinz, M. Ogawa, A. Makishima, S. Ichikawa, M. Itoh, M. Ishii, and J. Blomqvist, Phys. Rev. Lett. **81**, 4100 (1998).

[35] C. J. Chiara, I. Stefanescu, W. B. Walters, S. Zhu, R. V. F. Janssens, M. P. Carpenter, R. Broda, B. Fornal, A. A. Hecht, N. Hoteling, E. G. Jackson, B. P. Kay, W. Królas, T. Lauritsen, E. A. McCutchan, T. Pawłat, D. Seweryniak, X. Wang, A. Wöhr, and J. Wrzesiński, Phys. Rev. C **85**, 024309 (2012).

[36] I. Stefanescu, G. Georgiev, D. L. Balabanski, N. Blasi, A. Blazhev, N. Bree, J. Cederkäll, T. E. Cocolios, T. Davinson, J. Diriken, J. Eberth, A. Ekström, D. Fedorov, V. N. Fedosseev, L. M. Fraile, S. Franchoo, K. Gladnishki, M. Huyse, O. Ivanov, V. Ivanov, J. Iwanicki, J. Jolie, T. Konstantinopoulos, T. Kröll, R. Krücken, U. Köster, A. Lagoyannis, G. Lo Bianco, P. Maierbeck, B. A. Marsh, P. Napiorkowski, N. Patronis, D. Pauwels, G. Rainovski, P. Reiter, K. Riisager, M. Seliverstov, G. Sletten, J. Van de Walle, P. Van Duppen, D. Voulot, N. Warr, F. Wenander, and K. Wrzosek, Phys. Rev. Lett. **100**, 112502 (2008).

[37] E. Sahin, M. Doncel, K. Sieja, G. de Angelis, A. Gadea, B. Quintana, A. Görgen, V. Modamio, D. Mengoni, J. J. Valiente-Dobón, P. R. John, M. Albers, D. Bazzacco, G. Benzoni, B. Birkenbach, B. Cederwall, E. Clément, D. Curien, L. Corradi, P. Désesquelles, A. Dewald, F. Didierjean, G. Duchêne, J. Eberth, M. N. Erduran, E. Farnea, E. Fioretto, G. de France, C. Fransen, R. Gernhäuser, A. Gottardo, M. Hackstein, T. Hagen, A. Hernández-Prieto, H. Hess, T. Hüyük, A. Jungclaus, S. Klupp, W. Korten, A. Kusoglu, S. M. Lenzi, J. Ljungvall, C. Louchart, S. Lunardi, R. Menegazzo, C. Michelagnoli, T. Mijatović, B. Million, P. Molini, G. Montagnoli, D. Montanari, O. Möller, D. R. Napoli, A. Obertelli, R. Orlandi, G. Pollarolo, A. Pullia, F. Recchia, P. Reiter, D. Rosso, W. Rother, M.-D. Salsac, F. Scarlassara, M. Schlarb, S. Siem, P. P. Singh, P.-A. Söderström, A. M. Stefanini, O. Stézowski, B. Sulignano, S. Szilner, C. Theisen, C. A. Ur, and M. Yalcinkaya, Phys. Rev. C **91**, 034302 (2015).

[38] N. J. Stone, K. van Esbroeck, J. R. Stone, M. Honma, T. Giles, M. Veskovic, G. White, A. Wöhr, V. I. Mishin, V. N. Fedoseyev, U. Köster, P. F. Mantica, and W. B. Walters, Phys. Rev. C **77**, 014315 (2008).

[39] C. J. Chiara, R. Broda, W. B. Walters, R. V. F. Janssens, M. Albers, M. Alcorta, P. F. Bertone, M. P. Carpenter, C. R. Hoffman, T. Lauritsen, A. M. Rogers, D. Seweryniak, S. Zhu, F. G. Kondev, B. Fornal, W. Królas, J. Wrzesiński, N. Larson, S. N. Liddick, C. Prokop, S. Suchyta, H. M. David, and D. T. Doherty, Phys. Rev. C **86**, 041304 (2012).

[40] I.-Y. Lee, Nucl. Phys. A **520**, c641 (1990).

[41] F. Ajzenberg-Selove, R. E. Brown, E. R. Flynn, and J. W. Sunier, Phys. Rev. C **24**, 1762 (1981).

[42] B. Zeidman and J. A. Nolen, Phys. Rev. C **18**, 2122 (1978).

[43] K. Sieja and F. Nowacki, Phys. Rev. C **81**, 061303 (2010).

[44] S. Suchyta, S. N. Liddick, Y. Tsunoda, T. Otsuka, M. B. Bennett, A. Chemey, M. Honma, N. Larson, C. J. Prokop, S. J. Quinn, N. Shimizu, A. Simon, A. Spyrou, V. Tripathi, Y. Utsuno, and J. M. Von Moss, Phys. Rev. C **89**, 021301 (2014).

[45] F. Recchia, C. J. Chiara, R. V. F. Janssens, D. Weisshaar, A. Gade, W. B. Walters, M. Albers, M. Alcorta, V. M. Bader, T. Baugher, D. Bazin, J. S. Berryman, P. F. Bertone, B. A. Brown, C. M. Campbell, M. P. Carpenter, J. Chen, H. L. Crawford, H. M. David, D. T. Doherty, C. R. Hoffman, F. G. Kondev, A. Korichi, C. Langer, N. Larson, T. Lauritsen, S. N. Liddick, E. Lunderberg, A. O. Macchiavelli, S. Noji, C. Prokop, A. M. Rogers, D. Seweryniak, S. R. Stroberg, S. Suchyta, S. Williams, K. Wimmer, and S. Zhu, Phys. Rev. C **88**, 041302 (2013).

[46] R. Broda, T. Pawłat, W. Królas, R. V. F. Janssens, S. Zhu, W. B. Walters, B. Fornal, C. J. Chiara, M. P. Carpenter, N. Hoteling, L. W. Iskra, F. G. Kondev, T. Lauritsen, D. Seweryniak, I. Stefanescu, X. Wang, and J. Wrzesiński, Phys. Rev. C **86**, 064312 (2012).

[47] N. Shimizu, T. Abe, Y. Tsunoda, Y. Utsuno, T. Yoshida, T. Mizusaki, M. Honma, and T. Otsuka, Prog. Theor. Exp. Phys **01A205** (2012).

[48] T. Otsuka, M. Honma, T. Mizusaki, N. Shimizu, and Y. Utsuno, Prog. Part. Nucl. Phys. **47**, 319 (2001).

[49] D. Pauwels, J. L. Wood, K. Heyde, M. Huyse, R. Julin, and P. Van Duppen, Phys. Rev. C **82**, 027304 (2010).

[50] M. P. Carpenter, R. V. F. Janssens, and S. Zhu, Phys. Rev. C **87**, 041305 (2013).

[51] H. L. Crawford, R. M. Clark, P. Fallon, A. O. Macchiavelli, T. Baugher, D. Bazin, C. W. Beausang, J. S. Berryman, D. L. Bleuel, C. M. Campbell, M. Cromaz, G. de Angelis, A. Gade, R. O. Hughes, I. Y. Lee, S. M. Lenzi, F. Nowacki, S. Paschalis, M. Petri, A. Poves, A. Ratkiewicz, T. J. Ross, E. Sahin, D. Weisshaar, K. Wimmer, and R. Winkler, Phys. Rev. Lett. **110**, 242701 (2013).